

Spin-cluster excitations in $\text{RbFeCl}_3 \cdot 2\text{H}_2\text{O}$

Q. A. G. van Vlimmeren, C. H. W. Swüste, and W. J. M. de Jonge
Physics Department, Eindhoven University of Technology, Eindhoven, The Netherlands

M. J. H. van der Steeg, J. H. M. Stoelinga, and P. Wyder
Research Institute for Materials, Physics Laboratory, University of Nijmegen, Toernooiveld, Nijmegen, The Netherlands
(Received 11 July 1979)

Spin-cluster excitations (SCE) from the ground state are observed in the pseudo-one-dimensional canted Ising antiferromagnet $\text{RbFeCl}_3 \cdot 2\text{H}_2\text{O}$. Since the moments are canted with respect to each other, SCE were observed which show characteristics of a ferromagnetic chain and an antiferromagnetic chain when the external field is along the c or a axis, respectively. The results cannot be interpreted with the simple Ising model as in the case of spin-cluster resonance (SCR) reported earlier. For the small spin clusters observed in the present experiment, it is necessary to include effects from the higher single-ion states. Together with SCR the data provide rather detailed information on the magnetic ground state and the interactions.

I. INTRODUCTION

The elementary magnetic excitations in an Ising system are not collective spin waves as in a Heisenberg system, but localized spin reversals called spin clusters or magnon bound states. An m -fold spin cluster $|m\rangle$ is defined as a cluster of m neighboring spins which are reversed with respect to their direction in the ground state.

Although spin clusters are expected to exist in all Ising-like systems at nonzero temperatures, they have been observed in only a few compounds. Direct excitation of spin clusters (SCE) have been observed and reported in $\text{CoCl}_2 \cdot 2\text{H}_2\text{O}$ (Ref. 1) and $\text{CoBr}_2 \cdot 2\text{H}_2\text{O}$ (Ref. 2). In a previous article³ (further referred to as I) we reported on the indirect observation of spin clusters in $\text{RbFeCl}_3 \cdot 2\text{H}_2\text{O}$ by inducing the transitions between spin clusters ($|m\rangle \rightarrow |m+n\rangle$) called spin-cluster resonance (SCR). Due to the pronounced one-dimensional character of this compound, the energy involved in these transitions is determined by only the relatively weak interchain interaction and therefore SCR can be observed in the gigahertz region. Due to the particular canted structure of the system, SCR could be observed which showed characteristic properties of a ferromagnetic chain and of an antiferromagnetic chain, depending on the orientation of the external magnetic field. It was shown that the results could be excellently explained assuming strongly anisotropic exchange interactions ($J^z \gg J^x, J^y$) and a small single-ion pseudodoublet ground-state splitting Δ , provided that only transitions between large spin clusters were observed. This last condition implies also that the effect of J^x and J^y , if present, and the shift of the levels caused by Δ could not be detected,

due to the drastic decrease of the influence of these terms on the transition frequencies between large spin clusters. In view of these arguments it seemed desirable to obtain additional information on the excitation spectrum and its field dependence of spin clusters of small size. This and the fact that the SCE spectrum of an antiferromagnetic Ising chain has not been reported before, motivated us to start an investigation of the direct excitation of spin clusters. In view of the large intrachain (~ 40 K) this implied the use of far-infrared spectroscopy.

In the next section we will review the experimental setup. Section III contains some relevant sample properties, while the basic theoretical background will be given in Sec. IV. Experimental results will be presented in Sec. V, and we will conclude with a discussion in Sec. VI.

II. EXPERIMENTAL

Single crystals of $\text{RbFeCl}_3 \cdot 2\text{H}_2\text{O}$ were grown by slow evaporation at 37°C from a solution of $\text{FeCl}_2 \cdot 4\text{H}_2\text{O}$ and RbCl in a molar ratio of 3.2:1. To prevent oxidation, a few drops of HCl were added to the solution which was kept in N_2 atmosphere. In this way large crystals ($2 \times 2 \times 0.5 \text{ cm}^3$) with well-developed crystal faces were obtained.

The far-infrared transmission experiments were performed in the region of $15\text{--}200 \text{ cm}^{-1}$ with a Grubb Parson's Michelson interferometer, operating with phase modulation at 13 Hz and modified to enable the use of a cooled Ge-bolometer as detector (see Fig. 1). Both the sample and the Ge-bolometer were at 1.2 K. This temperature warrants both an optimum bolometer performance and an optimum

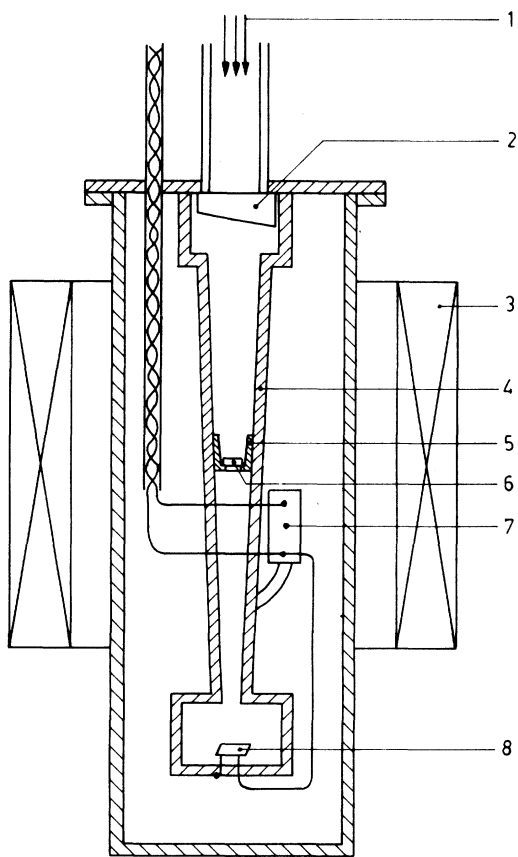


FIG. 1. Detector assembly, showing the position of the sample: (1) incident radiation, (2) low-temperature filter, (3) superconducting magnet, (4) light cone, (5) sample holder, (6) sample, (7) load resistor (1.5 M Ω), and (8) germanium bolometer.

signal shape for the spin-cluster excitations. The samples used in the experiments were about 1 mm thick. This thickness was experimentally found to yield the best transmission spectra. To improve the spectral resolution, single-sided interferograms were recorded, resulting in a resolution of 0.3 cm⁻¹. The interferogram output data were punched on tape and subsequently handled on a PDP-11 laboratory computer by a program with various facilities for manipulating interferograms and spectra.

The frequency-field dependence of the absorptions were obtained by making interferograms at several fixed magnetic fields. The magnetic field was produced by a small superconducting solenoid (Fig. 1).

III. PHYSICAL PROPERTIES

RbFeCl₃·2H₂O (RFC) belongs to a series of well-known isomorphous transition-metal halides $AMB_3 \cdot 2H_2O$ ($A = Cs, Rb$; $M = Mn, Co, Fe$;

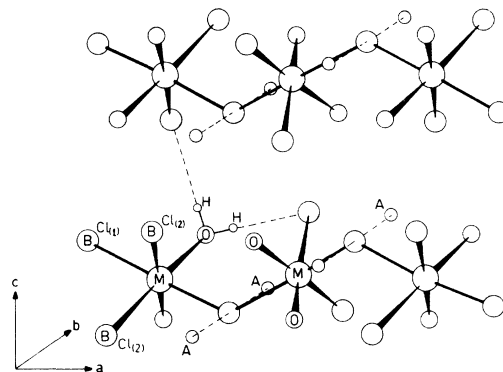


FIG. 2. Schematic representation of the crystallographic structure of $AMB_3 \cdot 2H_2O$ with $A = Rb$, $M = Fe$, and $B = Cl$. Only one set of hydrogens and hydrogen bonds is shown.

$B = Cl, Br$). A schematic drawing of the structure is shown in Fig. 2. All members of this series show pronounced linear-chain ($d = 1$) characteristics.⁴⁻⁶ In RbFeCl₃·2H₂O the (small) interchain interactions give rise to a magnetically ordered phase below $T_N = 11.96$ K.⁵ The resulting compensated four-sublattice magnetic array can be described⁷ by the space group $P_{2_1}c'ca$ and is shown in Fig. 3. This space group allows a canting of the magnetic moments in the ac plane resulting in a net magnetization of an individual chain in the c direction. Application of an external field along the c direction yields a phase diagram schematically shown in Fig. 4. The two metamagnetic transitions between antiferro-ferri and ferri-ferromagnetic are associated with a reorientation of the ferromagnetic components of the chains. The ground-state spin configurations, i.e., the spin

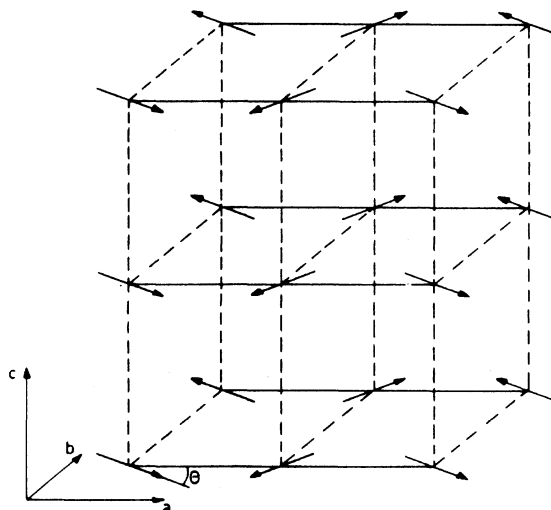


FIG. 3. Array of the magnetic moments in the ordered state. All moments are located in the ac plane at an angle θ from the a axis.

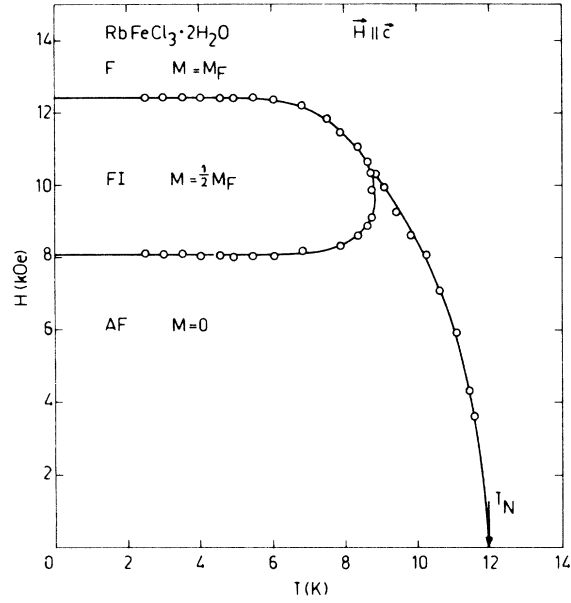


FIG. 4. Magnetic phase diagram of $\text{RbFeCl}_3 \cdot 2\text{H}_2\text{O}$ for $\vec{H} \parallel \vec{c}$. AF is the antiferromagnetic state, while FI and F denote the ferrimagnetic and ferromagnetic ordering between the ferromagnetic moments of the chains, respectively. M_F is the magnetization in the ferromagnetic phase. The curves are drawn as a guide to the eye.

configurations having the lowest energy at zero temperature in a magnetic field, can be determined by the method of Kudō and Katsura.⁸ The resulting arrays of the ferromagnetic components of the chain are given in Fig. 5. For the ferrimagnetic (FI) phase three different, although energetically equivalent spin configurations can be derived.

Information about the single-ion ground state and the exchange interactions has been obtained from susceptibility,⁹ specific-heat,⁵ spin-cluster-resonance,³ and Mössbauer experiments.¹⁰ The single-ion ground state can be described as a pseudodoublet with an energy separation of about 0.7 K. The remaining spin levels are situated at at least 40 K above this doublet, thus bringing about a rather Ising-like behavior of the system. At low temperatures the intrachain exchange has been estimated as $J/k = -39$ K, and the combined intrachain interaction as $J'/k = -0.7$ K.

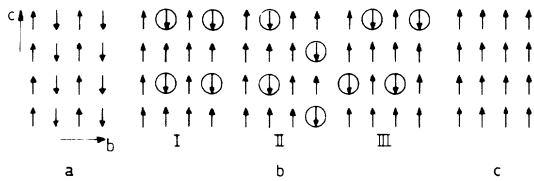


FIG. 5. Arrays of the ferromagnetic components of the chains. (a) Antiferromagnetic arrays of the chains. (b) Three possible ferrimagnetic arrays (the down moments are circled). (c) Ferromagnetic array.

IV. THEORY

An extensive theoretical treatment of the canted antiferromagnetic chain has been given in Paper I.³ Referring to that treatment, we quote for the Hamiltonian describing this system in the fictitious spin $S = \frac{1}{2}$ formalism [Eqs. (5.3), (5.8), and (5.9) in Paper I]:

$$H = H_e + H_\Delta + H_z + H_{ic} \quad (1)$$

which represent, respectively, the intrachain interactions, the single-ion effect, the Zeeman interactions, and the interchain interactions:

$$\begin{aligned} H_e = & -2J_a^z \sum_{j=1}^N S_j^z S_{j+1}^z \\ & - J_a^- \sum_{j=1}^N (S_j^+ S_{j+1}^+ + S_j^- S_{j+1}^-) \\ & - J_a^+ \sum_{j=1}^N (S_j^+ S_{j+1}^- + S_j^- S_{j+1}^+) \end{aligned} \quad (2a)$$

$$\text{with } J_a^- = \frac{1}{2}(J_a^{xx} - J_a^{yy}), \quad J_a^+ = \frac{1}{2}(J_a^{xx} + J_a^{yy});$$

$$H_\Delta = -\Delta S^x, \quad (2b)$$

$$\text{with } \Delta = 2D \{1 - [1 + 3(E/D)^2]^{1/2}\};$$

$$\begin{aligned} H_z = & -\mu_B g_{xx} H_x'' \sum_{j=1}^N \frac{1}{2} (S_j^+ + S_j^-) \\ & - \mu_B g_{zx} H_x'' \sum_{j=1}^N (-1)^{j+1} S_j^z \\ & - \mu_B g_{xz} H_z'' \sum_{j=1}^N (-1)^{j+1} \frac{1}{2} (S_j^+ + S_j^-) \\ & - \mu_B g_{zz} H_z'' \sum_{j=1}^N S_j^z - \mu_B g_{yy} H_y'' \sum_{j=1}^N \frac{1}{2i} (S_j^+ - S_j^-) \end{aligned} \quad (2c)$$

$$H_{ic} = - \sum_{j=1}^N (-1)^{j+1} H_e S_j^z, \quad (2d)$$

with $H_e = \alpha J_b + \beta J_c + \gamma J_{bc}$ and $\alpha = 2, 0, \text{ or } -2$; $\beta = 2, 0, \text{ or } -2$; $\gamma = 4, 2, 0, -2, \text{ or } -4$. In these equations $x_j, y_j,$ and z_j refer to the local axis system in which $\langle \vec{S}_j \rangle$ is directed along z_j , while $x'', y'',$ and z'' are equivalent to the crystallographic axes $a, b,$ and c . For further details the reader is referred to Paper I.

Adapting the Ising-basic-function approach for the antiferromagnetic chain, the energy levels of spin clusters $|\pm m\rangle$ can now be calculated (the plus and minus sign in $|\pm m\rangle$ are related to the sign of the antiferromagnetic component of the spin cluster, i.e., the component along the a axis).

In Fig. 6 we have plotted the energy of the lowest spin clusters as a function of field for the two distinct cases with $\vec{H} \parallel \vec{c}$ ("ferromagnetic" chain) and $\vec{H} \parallel \vec{a}$

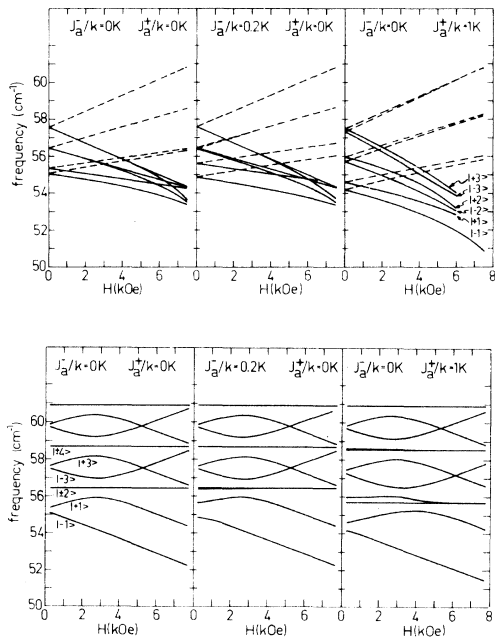


FIG. 6. Influence of J_a^- and J_a^+ on the excitation spectrum with $J_a^{zz} = -39$ K, $\Delta = 0.76$ K, and $H_e = 1.62$ K. The labeling refers to the drawn lines. (a) $\vec{H} \parallel \vec{c}$. The dashed lines refer to the spin-cluster energy levels for a chain with the total magnetic moment reversed with respect to the magnetic field. (b) $\vec{H} \parallel \vec{a}$.

("antiferromagnetic" chain). Only the excitations in the ground-state configuration are calculated [i.e., for the antiferromagnetic phase we have taken $\alpha = -2$, $\beta = 2$, and $\gamma = -4$ in Eq. (2)]. The figure shows the calculated effect of J_a^+ and J_a^- (which, as we mentioned before, are not known) and Δ on the lower levels. The other parameters were taken from the spin-cluster-resonance results. It can be seen that the influence of J_a^+ , J_a^- , and Δ terms, which can be considered as perturbations of the pure Ising case, becomes appreciable for small clusters, as was already stated in the Introduction.

It is important to note also that the action of J_a^+ and Δ [see Eq. (1)] couples the states with $\Delta m = 2$ and $\Delta m = 1$, respectively, and therefore allows higher-spin clusters to be observed, that is, in principle, when the energy difference between successive excitations is not too large.

V. RESULTS AND INTERPRETATIONS

In Fig. 7 a typical transmission spectrum of $\text{RbFeCl}_3 \cdot 2\text{H}_2\text{O}$ as a function of the frequency at zero magnetic field is shown. Since the spectrum is rather complicated, we will only consider the absorptions which show a dependence on the external magnetic field. Figures 8 and 9 show field-dependent absorptions near 50 cm^{-1} for $\vec{H} \parallel \vec{c}$ and $\vec{H} \parallel \vec{a}$, respectively.

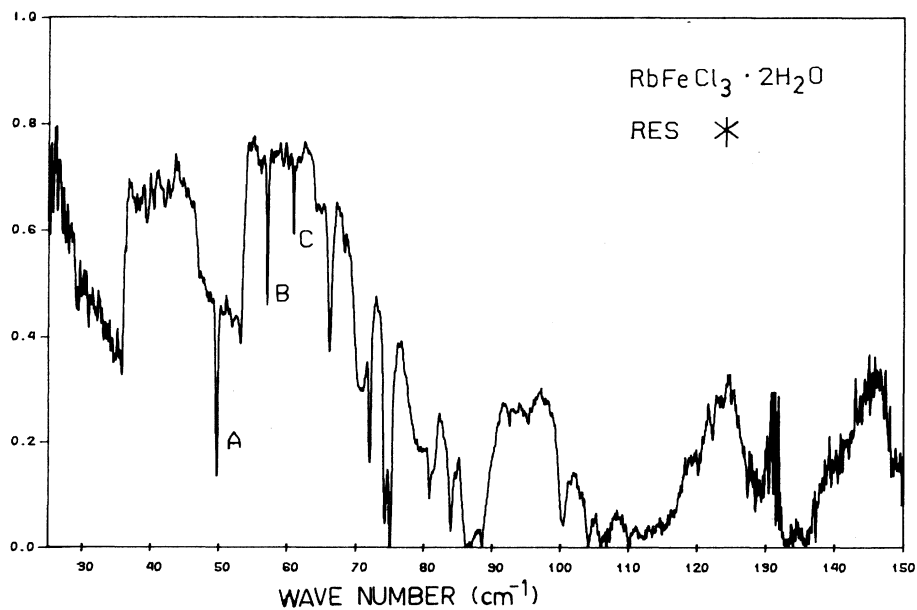


FIG. 7. A typical transmission spectrum T of $\text{RbFeCl}_3 \cdot 2\text{H}_2\text{O}$ relative to the transmission without specimen T_0 , as a function of the frequency in zero magnetic field at $T = 1.2$ K. The absorptions A and C are referred to in the text. The experimental resolution is 0.3 cm^{-1} .

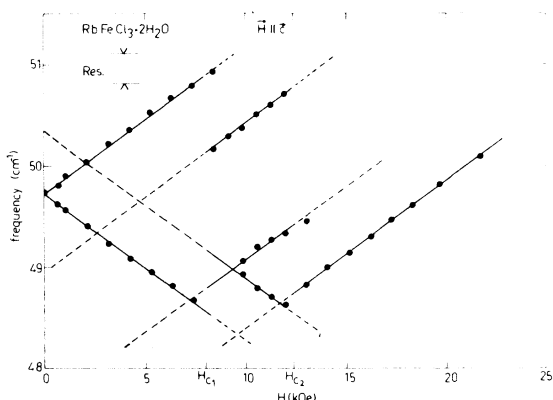


FIG. 8. The resonance frequency of absorption *A*, see Fig. 7, vs the magnetic field *H*, for $\vec{H} \parallel \vec{c}$. The lines are the theoretical predictions given in the text. H_{c1} and H_{c2} are the two critical fields. The experimental resolution is indicated by Res.

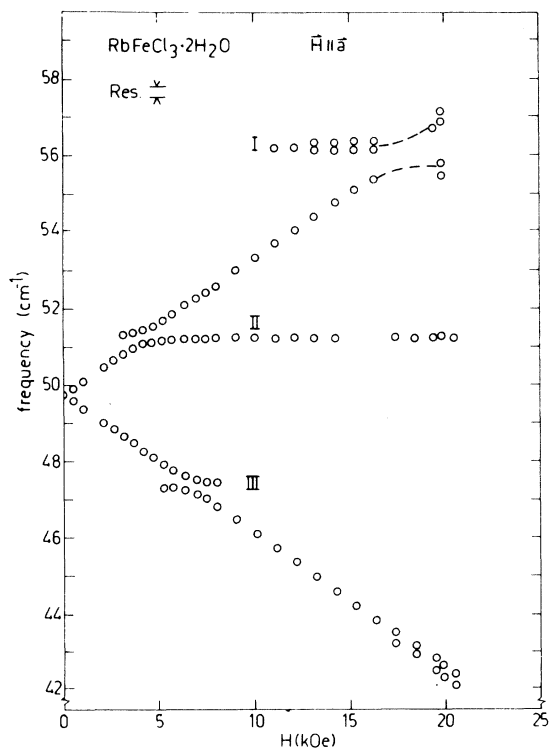


FIG. 9. The resonance frequency of absorption *A*, see Fig. 7, vs the magnetic field *H*, for $\vec{H} \parallel \vec{a}$. Three additional field-independent absorptions are labeled with Roman numerals. The slight splitting of absorption I and the two field-dependent absorptions at higher magnetic fields can be explained by a misorientation of the crystal by about 3° . The broken lines are drawn to indicate that the energy levels of the upper two absorptions do not intersect.

In zero field, part of these absorptions may be identified with the absorption marked by *A* in Fig. 7. The experimental linewidth of the absorption *A* equals the experimental resolution of 0.3 cm^{-1} . The central position of the absorption can be determined with an accuracy of 0.1 cm^{-1} .

From the value of the excitation energy (50 cm^{-1}) and the field dependence for $\vec{H} \parallel \vec{a}$ and $\vec{H} \parallel \vec{c}$, it is reasonable to assume that the absorption line *A* is a onefold spin-cluster excitation. At first sight no multiple-spin-cluster excitations are observed, with the possible exceptions of one or more of the field-independent absorptions marked by I, II, and III in Fig. 9, which show some peculiar repulsion effects and might be identified as excitations of spin clusters with an even number of spins (see Fig. 6). We will first investigate whether one of these can be identified as a twofold spin-cluster excitation.

The twofold spin-cluster-excitation energy is field independent for the magnetic field exactly parallel to the *a* axis (or in the *ab* plane). When this is not the case, a field dependence may be anticipated, due to the coupling of the magnetic field with the ferromagnetic *c* components of the magnetic moments. Note that the effect of this coupling has a different sign for neighboring chains which are antiferromagnetically coupled. Therefore, a splitting of the original signal ($\vec{H} \parallel \vec{a}$) will result. We have measured additional spectra with the magnetic field in the *ac* plane directed 6° from the *a* axis. These spectra showed unambiguously only a splitting of absorption I, having the expected order of magnitude. The other field-independent absorptions II and III are therefore identified as phonons, which interact with the onefold spin-cluster excitation.¹¹

Having identified the twofold spin-cluster excitation, the question remains why this excitation cannot be observed in zero magnetic field. This question is closely related to the fact that the intensity of the absorption of the twofold spin-cluster excitation is field dependent (illustrated by the absence of data points in Fig. 9 for $H < 10 \text{ kOe}$) and reaches a maximum value near the fictitious level crossing of the energy levels of the one- and twofold spin clusters. The exchange term J_a^+ cannot account for this mechanism, because the action of J_a^+ mixes the ground state and the twofold spin cluster. This would result in a *field-independent* contribution to the intensity of the twofold spin-cluster excitation. From the fact that at zero field the twofold spin-cluster excitation is not observed, it is clear that this contribution can be neglected. The field dependence of the intensity of the twofold spin-cluster excitation clearly indicates that an interaction term between the one- and twofold spin clusters plays an important role. In the preceding section the crystal-field term Δ has already been identified as such a term.

At this stage it is not difficult to realize that the

m -fold spin-cluster excitations with $m \geq 2$ could not be observed in the experiments with the magnetic field along the c axis, since the energy levels of the one- and twofold spin clusters do not intersect for $\vec{H} \parallel \vec{c}$ as can be seen in Fig. 6.

From Fig. 9 it can be deduced that at zero field the excitation of the one- and twofold spin cluster requires an energy of 49.7 and 56.2 cm^{-1} , respectively. The resulting energy difference of 6.5 cm^{-1} between the one- and twofold spin-cluster excitations at zero field, however, is much larger than the value of the interchain coupling 1.6 K ($\approx 1.1 \text{ cm}^{-1}$) expected from the Ising prediction. Moreover, the difference cannot be explained by taking into account the non-Ising terms Δ , J_a^+ , and J_a^- . At zero field the effect of the pseudodoublet splitting, Δ , on the energy levels of the one- and twofold spin clusters is small ($\approx 0.2 \text{ cm}^{-1}$), as is shown in Fig. 6. The anisotropic exchange term J_a^+ is expected to be small, as was shown above, while J_a^- would split up the onefold spin-cluster excitation in zero field, as can be inferred from Fig. 6, which effect is not observed in the experiments.

However, we have to realize that so far we have used the effective $S = \frac{1}{2}$ spin Hamiltonian and have not taken into account a possible mixing of higher-energy states into both the ground state and spin-cluster states due to the exchange coupling. All the results so far reported here and in Paper I showed that this effect did not hamper an interpretation in terms of the $S = \frac{1}{2}$ spin Hamiltonian formalism. We will show that this is caused by the fact that only the behavior of large spin clusters has been observed. It can be argued in an intuitive way that in a certain sense the onefold spin cluster is an exception. Consider for sake of simplicity a ferromagnetic $S = \frac{1}{2}$ Ising chain. All spins will be parallel in the ground state, i.e., $|m_s = \frac{1}{2}\rangle$ at zero temperature. In the Ising case the total energy of the system is the sum of the single spin energies. The spins experience an "exchange field" $H_e = J$ from their neighbor spins in the chain, yielding a single spin energy-level scheme as is shown in Fig. 10. In this figure we have also indicated the energies of the spins in the ground state and in a one-, a two-, and a fourfold spin cluster. It is obvious that only for the onefold spin cluster the highest-energy level C is occupied. In an analogous way it can be shown that the same difference exists in the antiferromagnetic Ising chain. Although this argument by itself does not explain the anomalous behavior, it may serve to indicate, however, a possible source of complications.

In order to obtain some quantitative results, we have performed perturbation calculations on the energies of the ground state and the onefold and multiple spin cluster states of a finite chain of n spins ($n > 4$) in the real spin $S = 2$. Assuming an isotro-

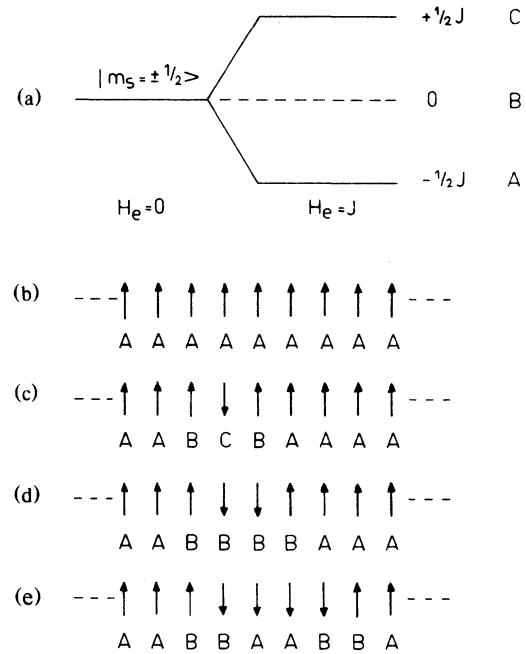


FIG. 10. Energy-level scheme of a spin $S = \frac{1}{2}$ in an "exchange field" J (a). In (b), (c), (d), and (e) the ground state, a onefold, a twofold, and a fourfold spin-cluster state are shown, respectively. The energy of each spin is indicated by A, B, and C corresponding to the energy levels shown in (a).

pic exchange interaction J in the real spin and neglecting—for sake of simplicity—the orthorhombic contribution to the crystal field, we obtain the following Hamiltonian

$$H = \sum_{j=1}^N \{ D[(S_j^z)^2 - \frac{1}{3}S(S+1)] - 2J^z z^j S_j^z S_{j+1}^z - J^+(S_j^+ S_{j+1}^- + S_j^- S_{j+1}^+) - J^-(S_j^+ S_{j+1}^+ + S_j^- S_{j+1}^-) - J^{as}[(S_j^+ + S_j^-)S_{j+1}^z - S_j^z(S_{j+1}^+ + S_{j+1}^-)] \} , \quad (3)$$

with

$$J^z z^j = J \cos 2\theta , \quad J^+ = \frac{1}{2}J(\cos 2\theta + 1) ,$$

$$J^- = \frac{1}{2}J(\cos 2\theta - 1) , \quad J^{as} = -J \sin 2\theta .$$

Here x' , y' , z' denotes the local coordinate system in which g is diagonal and θ is the angle between the z' and the a axis.

The energy difference between the one- and twofold spin-cluster-excitation energies is obtained from second-order perturbation calculations in which the

effect of J is considered as the perturbation. The result is

$$E_1 - E_2 = (4J^+)^2 \left(\frac{-2}{6D + 2Jz'z'} + \frac{2}{6D + 10Jz'z'} \right) + (4J^-)^2 \left(\frac{1}{6D - 10Jz'z'} - \frac{1}{6D - 2Jz'z'} \right) + (J^{as})^2 \left(\frac{64}{3D + 8Jz'z'} + \frac{64}{3D - 8Jz'z'} \right). \quad (4)$$

These calculations showed also that the effect of the exchange coupling with higher states is almost the same for the multiple spin-cluster excitations, $m \geq 2$, which corroborates the fact that this effect was not observed in the spin-cluster resonance experiments. Using Eq. (4) and inserting the values $D/k = -20$ K, $E/k = 0$ K, $J/k = -3.2$ K ($S = 2$), and $\theta = 20^\circ$, obtained from various experiments,⁹ an energy difference between the one- and twofold spin-cluster-excitation energies of 7 cm^{-1} is obtained. Given the uncertainty in the parameters, this value is in fair agreement with the experimentally observed energy difference 5.4 cm^{-1} . (Note that this value is the experimentally observed energy difference of 6.5 cm^{-1} corrected for the interchain coupling, which amounts to 1.1 cm^{-1} .) The perturbation calculation shows also that the estimate for J_a^z obtained from the onefold spin-cluster excitation will be about 2% too low. Further, the perturbation calculation predicts a reduction of the magnetic moment at zero external field of about 8% for the onefold spin cluster, while it is negligible for the multiple spin clusters. Since the spin-cluster resonances were explained as transitions between large spin clusters, the spin-cluster resonances give the correct value for the magnetic moment, $\mu = 4.5 \mu_B$ (Paper I). Comparing this value with the magnetic moment $\mu = 4.2 \mu_B$ found by the far-infrared experiment for the onefold spin-cluster excitation, we may conclude that the observed reduction of the magnetic moment (7%) is in fair agreement with the reduction predicted by the perturbation calculations ($\approx 8\%$).

In Fig. 9 a linear field dependence is observed for the onefold spin-cluster excitation, with the obvious exception of the effect of the interactions with the twofold spin-cluster excitation and optical phonons. Hence we may conclude that a magnetic field has no appreciable effect on the perturbed states and the magnetic moment for the onefold spin-cluster excitation as derived above.

The same conclusion can be drawn for the spectrum with $\vec{H} \parallel \vec{c}$, Fig. 8, in which a linear field dependence of the absorption frequencies is observed. The relative position of the absorption lines with respect to each other (Fig. 8) yield information about the interchain exchange interactions. The absolute fre-

quency of the absorption lines is determined by the—slightly modified—intrachain interaction.

In order to compare the results for $\vec{H} \parallel \vec{c}$ with the spin-cluster-resonance experiments we fitted the data of the excitations in the ground-state spin configurations of the various magnetic phases to the predictions of a spin $S = \frac{1}{2}$ model [see also Eq. (3.7) in Paper I]. This yielded $J_a^z/k = -35.0$ K, $J_b/k = -0.7$ K, $J_c/k = -0.2$ K, $J_{bc}/k = -0.13$ K, and $\mu_c = 1.6 \mu_B$. The drawn lines in Fig. 8 represent these predictions. In the fitting procedure we have made use of the fact that two absorptions are observed in more than one magnetic phase, viz., at 8.4 and 13 kOe. This yielded a demagnetizing field of 400 Oe in the ferrimagnetic phase and 800 Oe in the ferromagnetic phase. Since the sample was rather platelike, the above values may be compared with the values calculated for an infinite plate, i.e., 490 Oe for the ferrimagnetic phase and 980 Oe in the ferromagnetic phase.

VI. DISCUSSION AND CONCLUSIONS

The spin-cluster excitations in the far-infrared region yielded information about the one- and twofold spin clusters. From these experiments it appeared that the onefold spin cluster is 6.5 cm^{-1} lower in energy than the twofold spin cluster. This has to be compared with the expected energy difference, 1.1 cm^{-1} , for the pure Ising case. The larger energy difference could satisfactorily be explained by considering the influence of higher-energy states in the $S = 2$ model.

Assuming that only the pseudodoublet splitting term Δ contributes to the repulsion between the one- and twofold spin-cluster excitation energies ($\vec{H} \parallel \vec{a}$), the value of Δ can be obtained from the inferred minimum frequency difference ($\epsilon \approx 0.6 \text{ cm}^{-1}$) between the onefold and twofold spin-cluster excitations (Fig. 9). Since $\epsilon = \sqrt{2}\Delta$, this yields $\Delta/k = 0.6$ K, which value compares favorably with the result (0.76 K) of the spin-cluster resonances. [In the calculation of the energy difference only the energy levels of $|-1\rangle$, $|-2\rangle$, and $|+2\rangle$ (see Fig. 10) are of importance yielding an expression for ϵ which differs from Eq. (5.17) in Paper I for the spin-cluster resonances.]

Only the onefold spin-cluster excitation is observed when the magnetic field is applied in the c direction. Fitting the experimental data to an $S = \frac{1}{2}$ model yielded values for several parameters. In Table I these results are compared with the results of the spin-cluster resonances and various other experimental techniques.

Combining the results of both the spin-cluster resonances and the spin-cluster excitations yields predictions for the spin-cluster-excitation energies for $\vec{H} \parallel \vec{c}$

TABLE I. Values of several parameters as determined by various experimental techniques.

Parameter	SCE	SCR	Other techniques
D/k			-21 K^a
E/k			$0 \text{ K},^a 1.4 \text{ K}^b$
Δ/k	0.6 K	0.76 K	0.3 K^b
$J_a^{zz}/k, S = \frac{1}{2}$	-35 K		-39 K^c
$J_a/k, S = 2$	-2.8 K^d		$-2.7 \text{ K},^a -3.2 \text{ K}^e$
J_b/k	-0.7 K	-0.76 K	
J_c/k	-0.2 K	-0.21 K	-0.22 K^e
J_{bc}/k	-0.13 K	-0.13 K	
$(J_b + 2J_{bc})/k$	-1.0 K	-1.02 K	-1.07 K^e
μ_c	$1.6 \mu_B$	$1.5 \mu_B$	$1.6 \mu_B^e$
μ	$4.2 \mu_B$	$4.5 \mu_B$	$4.6 \mu_B,^f 3.9 \mu_B^g$
θ_m	22°	19°	$19^\circ,^f 16^\circ^g$

^aHigh temperature susceptibility; for susceptibility and magnetization measurements, see Ref. 9.

^bLow temperature susceptibility; for susceptibility and magnetization measurements, see Ref. 9.

^cMagnetic specific heat, Ref. 4.

^d $\theta = \theta_m = 20^\circ$.

^eMagnetization measurements; for susceptibility and magnetization measurements, see Ref. 9.

^fNuclear magnetic resonance, Ref. 11.

^gNeutron diffraction, Ref. 11.

and $\vec{H} \parallel \vec{a}$ which are presented in Fig. 11. The drawn curves in this figure represent the excitation energies for: $J_a^{zz}/k = -35.0 \text{ K}$, $J_a^+/k = 0 \text{ K}$, $J_a^-/k = 0 \text{ K}$, $J_b/k = -0.76 \text{ K}$, $J_c/k = -0.21 \text{ K}$, $J_{bc}/k = -0.13 \text{ K}$, $E_2 - E_1 = 9.4 \text{ K}$, $\mu = 4.1 \mu_B$, and $\theta_m = 20^\circ$ for the one-fold spin cluster, $\mu = 4.5 \mu_B$ and $\theta_m = 20^\circ$ for the multiple spin clusters, and $\Delta/k = 0.76 \text{ K}$. The coupling

of the onefold spin-cluster excitation with the optical phonons is not taken into account. The effect of the downward shift of the onefold spin-cluster-excitation energy for $\vec{H} \parallel \vec{a}$ can be obtained by comparing Fig. 11 with Fig. 6 or with Fig. 7 in Paper I.

In the experiments with $\vec{H} \parallel \vec{a}$ also the twofold spin-cluster excitation was observed, which can be

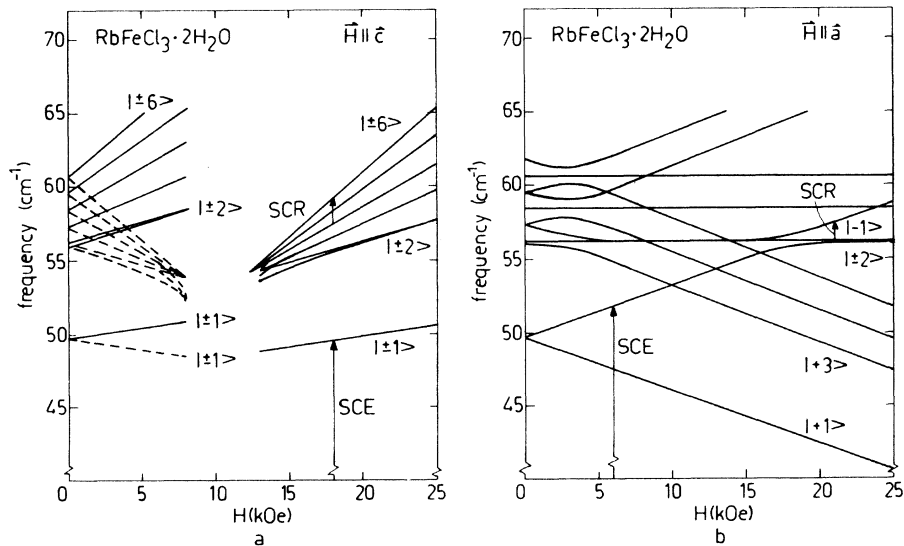


FIG. 11. The excitation energies of the spin clusters $|\pm 1\rangle$ to $|\pm 6\rangle$ for $\vec{H} \parallel \vec{c}$ (a) and $\vec{H} \parallel \vec{a}$ (b). These predictions for the excitation spectra are based on both the spin-cluster resonance and spin-cluster excitation results. The parameter values are given in the text. The broken lines in (a) represent excitations in a chain with a total chain moment antiparallel with respect to the field.

excited due to a magnetic-field-dependent coupling with the onefold spin cluster by the crystal-field term Δ . From the fact that the twofold spin-cluster excitation is only observable because of its mixing with the onefold spin cluster, it was inferred that $J_a^+/J_a^- \ll 1$, confirming once again the strong anisotropic character of $\text{RbFeCl}_3 \cdot 2\text{H}_2\text{O}$ at low temperatures.

Given the field dependence of the one- and twofold spin-cluster excitations for $\vec{H} \parallel \vec{a}$ presented in Figs. 9 and 11 one may conjecture that transitions between the one- and twofold spin clusters should be observable in our experiments for magnetic fields > 10 kOe and in the frequency region given approximately by $E_2 - E_1 < 2 \text{ cm}^{-1} \approx 60 \text{ GHz}$. No spin-cluster-resonance data in this field region, $\vec{H} \parallel \vec{a}$, were presented in Paper I, although at fields higher than 8 kOe very weak absorptions were observed. An analysis of these weak absorptions showed that they represent the transitions between the one- and twofold spin clusters indeed. In Fig. 12 these spin-cluster resonances are shown (open circles) together with the energy differences between the experimentally observed one- and twofold spin-cluster excitations presented in Fig. 9 (solid circles). Moreover, the prediction for the transition energy between the one- and twofold spin clusters based on the results presented in Fig. 11 is shown. The agreement between the spin-cluster-resonance data and the far-infrared measurements is satisfying. Although not all parameters which determine the intensity of the spin-cluster resonances (like the cluster distribution for $\vec{H} \parallel \vec{a}$) are known, the very small intensity of the spin-cluster resonances presented in Fig. 12 confirms that the spin-cluster resonances presented in Paper I contain the contributions of a large number of spin clusters with different cluster size.

As we saw in Fig. 9 the onefold spin-cluster excitation also shows interactions with two optical phonons, giving rise to hybridization of the phonon and the onefold spin-cluster excitation in the spectra for $\vec{H} \parallel \vec{a}$. The phonon energies, 47.4 and 51.2 cm^{-1} , are somewhat larger than the energies of the optical phonons observed in $\text{CoCl}_2 \cdot 2\text{H}_2\text{O}$ (29.3 cm^{-1})¹ and $\text{FeCl}_2 \cdot 2\text{H}_2\text{O}$ (31.5 cm^{-1})². The magnon-phonon coupling constants are 0.3 K for phonon II and 0.25 K for phonon III (see Fig. 9). These values are of the same order of magnitude as was found for $\text{CoCl}_2 \cdot 2\text{H}_2\text{O}$ (0.8 K) and $\text{FeCl}_2 \cdot 2\text{H}_2\text{O}$ (1.4 K). The values of the phonon energies and the magnon-phonon coupling constants indicate that the optical phonon observed in $\text{RbFeCl}_3 \cdot 2\text{H}_2\text{O}$ correspond to vibrations of the water molecules with respect to the Fe^{2+} ion.

The absorption A in Fig. 7 is not the only field-dependent absorption, but at higher frequencies field-dependent absorptions are observed also, i.e., near 75 and 100 cm^{-1} . The field dependence of the absorption frequencies is small for $\vec{H} \parallel \vec{c}$ and could

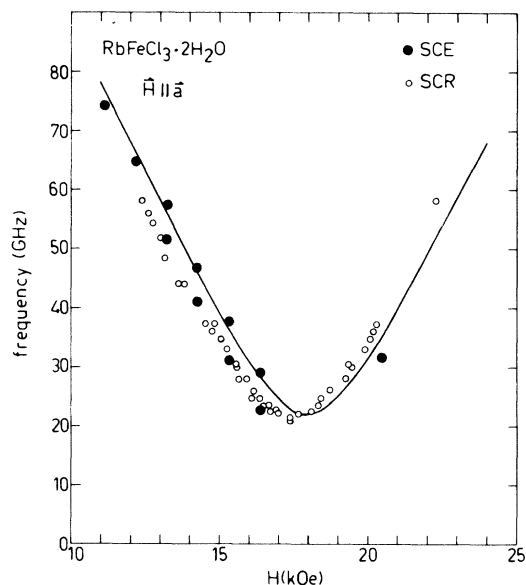


FIG. 12. Observed spin-cluster-resonance frequencies vs the magnetic field H ($H > 10$ kOe), for \vec{H} along the a axis (open circles). The prediction from the far-infrared experiments is obtained from the energy difference between actually observed one- and twofold spin-cluster excitations (solid circles). The curve denotes the calculated behavior for $\mu = 4.1 \mu_B$, $\theta_m = 20^\circ$, $E_2 - E_1 = 6.5 \text{ cm}^{-1}$ at zero field, and $\Delta/k = 0.76 \text{ K}$.

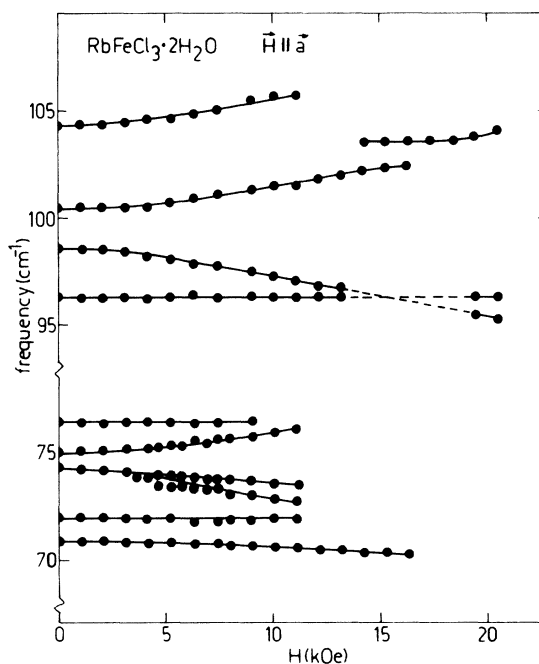


FIG. 13. The field dependence of the absorption frequency of a number of absorptions in the frequency regions 70–77 cm^{-1} and 95–105 cm^{-1} . The curves are drawn as a guide to the eye. Note the discontinuity in the frequency axis.

not be resolved. When the magnetic field is applied along the a axis, however, the absorption frequencies depend much more on the magnetic field as is shown in Fig. 13. Probably these excitations correspond to higher excited states of the spin quintet, drastically modified by the exchange interaction.

Furthermore, the typical field dependence of the intensity of absorption B and C (Fig. 7) has to be mentioned. Although the frequencies of the absorptions B and C do not depend on the magnetic field, their intensities depend strongly on the phase of the magnetic system, $\vec{H} \parallel \vec{c}$, in which they are observed. The intensities in the ferrimagnetic phase are one half of the intensities in the antiferromagnetic phase, while the intensities are zero in the ferromagnetic phase. As the frequencies of the absorptions B and C are field independent, it is expected that they are phonons. Yet, the mechanism which is responsible for the typical behavior of their intensities is not known. The value of the intensities in the ferrimagnetic phase suggests that the magnetization or the ordering pattern is of importance. Nevertheless, this phenomenon confirms the existence of a coupling between phonons and the magnetic system.

In conclusion, one may state that the present far-infrared study of the excitation spectrum has yielded

a large amount of detailed data about the local interaction parameters and the ground state, as is shown in Table I. Moreover, the excitation spectrum of the antiferromagnetic chain could be observed. However, one of the original aims of these investigations, that is the observation of the expected effect of J_a^+ , J_a^- , and Δ on specific small clusters, has been achieved only partially. Although it could be deduced from the experimental data that both perturbations from the pure Ising Hamiltonian must be very small indeed, an accurate estimate could not be given due to the unexpected large influence of higher single-ion states on the lowest spin-cluster excitations.

ACKNOWLEDGMENTS

The authors wish to acknowledge K. Kopinga for his continuous interest and valuable contributions and H. Hadders for the preparation of the crystals. One of the authors (Q.A.G.v.V.) wishes to thank the members of the experimental physics group of Nijmegen for their hospitality during his stay. This investigation is part of the research program of the Stichting voor Fundamenteel Onderzoek der Materie (FOM).

-
- ¹J. B. Torrance and M. Tinkham, *J. Appl. Phys.* **39**, 822 (1968); *Phys. Rev.* **187**, 587,595 (1969); D. F. Nicoli and M. Tinkham, *Phys. Rev. B* **9**, 3126 (1974).
²J. B. Torrance and K. A. Hay, *Phys. Rev. Lett.* **31**, 163 (1973).
³Q. A. G. van Vlimmeren and W. J. M. de Jonge, *Phys. Rev. B* **19**, 1503 (1979).
⁴K. Kopinga, *Phys. Rev. B* **16**, 427 (1977).
⁵K. Kopinga, Q. A. G. van Vlimmeren, A. L. M. Bongaarts, and W. J. M. de Jonge, *Physica (Utrecht)* **86-88 B+C**, 671 (1977).

- ⁶K. Kopinga, Ph.D. thesis (Eindhoven, 1976) (unpublished).
⁷J. A. J. Basten, Q. A. G. van Vlimmeren, and W. J. M. de Jonge, *Phys. Rev. B* **18**, 2179 (1978).
⁸T. Kudō and S. Katsura, *Prog. Theor. Phys.* **56**, 435 (1976).
⁹Q. A. G. van Vlimmeren, Ph.D. thesis (Eindhoven, 1979) (unpublished).
¹⁰H. Th. le Fever, *J. Magn. Magn. Mater.* (to be published).
¹¹See also Refs. 1 and 2.